

Supporting information

Food-Additive-Inspired Bifunctional Proton Buffering-Iron Capture Route to Low-Defect Prussian Blue Cathodes for Sodium-Ion Batteries

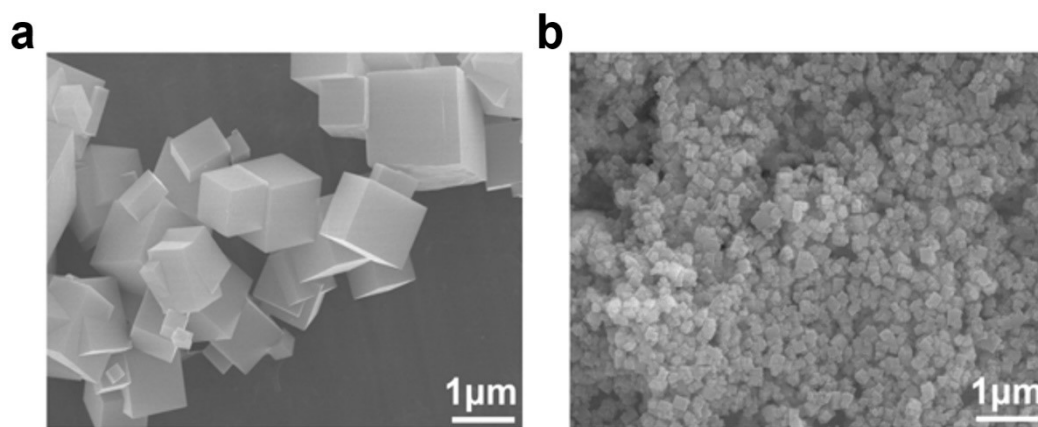


Fig. S1 SEM images of (a) PB, and (b) InsP₆-PB-30.

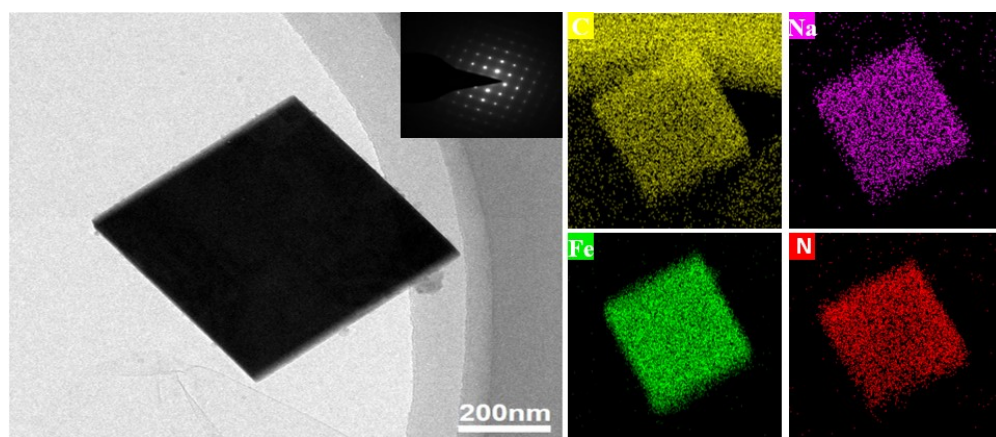


Fig. S2 TEM image of InsP₆-PB-10 and the corresponding EDX mapping images.

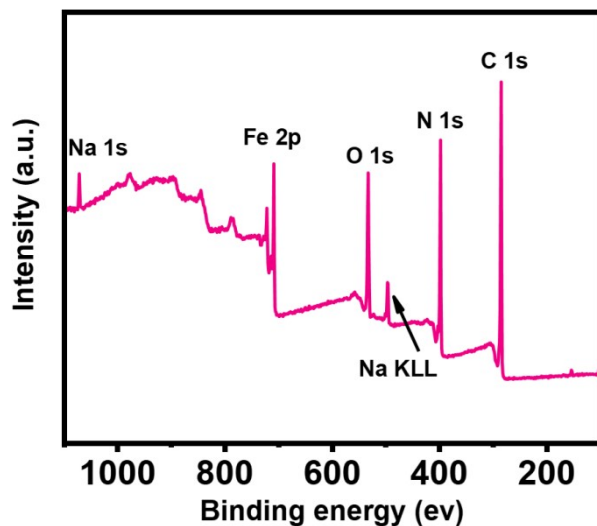


Fig. S3 XPS spectrum of InsP₆-PB-10.

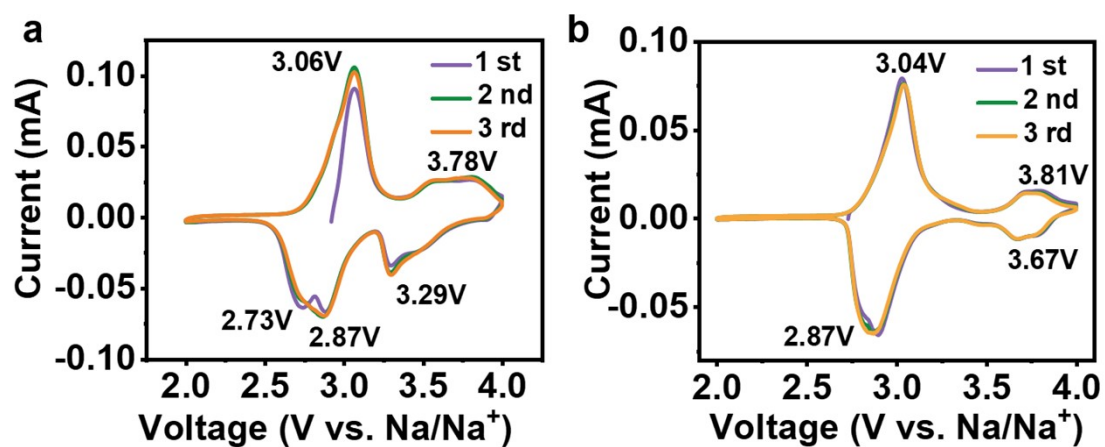


Fig. S4 CV curves at 0.1 mV s^{-1} of (a) InsP₆-PB-30, and (b) PB.

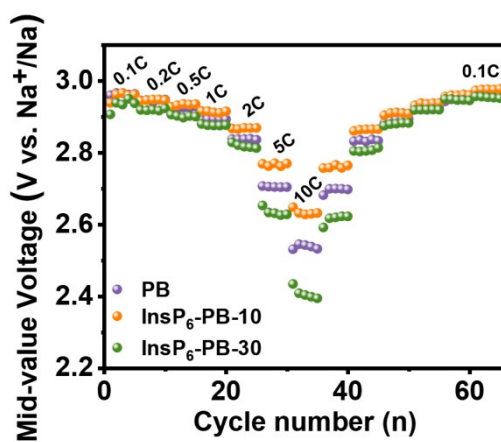


Fig. S5 Mid-value voltage of the samples at different current densities.

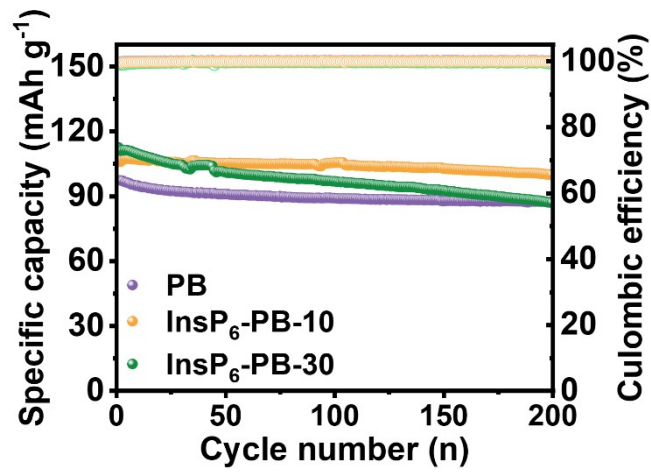


Fig. S6 Cycling performance at 1 C.

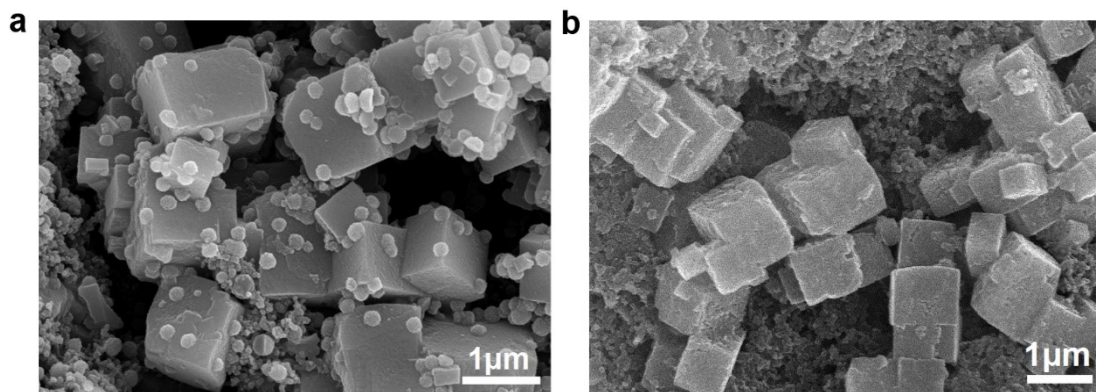


Fig. S7 SEM images of $\text{InsP}_6\text{-PB-10}$ (a) before, and (b) after 200 cycles.

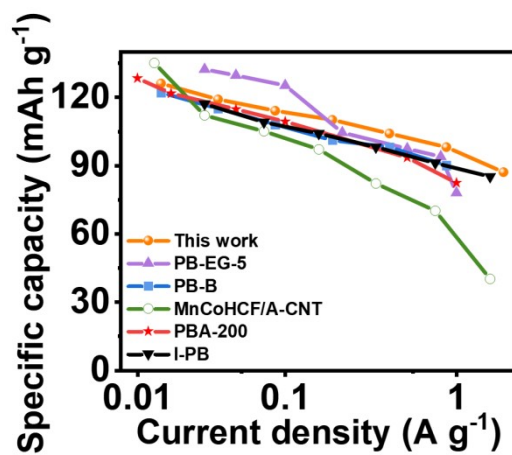


Fig. S8 The rate performance comparison with the recent PB electrodes.

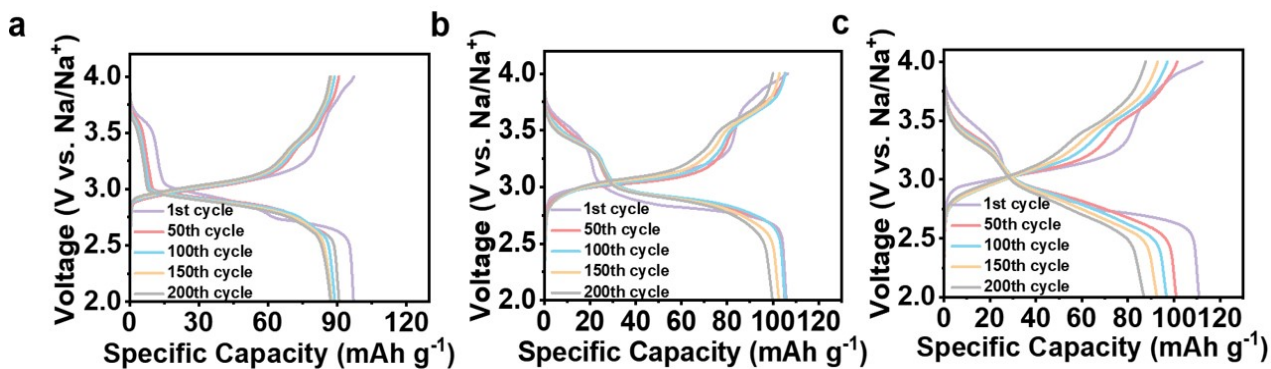


Fig. S9 Charge-discharge profiles at 1C of (a) PB, (b) InsP₆-PB-10, and (c) InsP₆-PB-30.

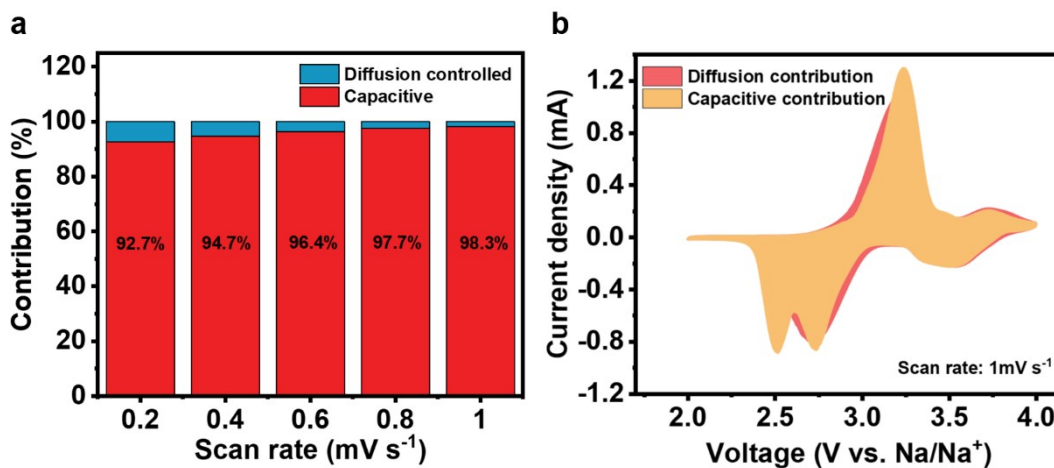


Fig. S10 (a) The proportion of the capacitance contribution at various scanning rates for InsP₆-PB-10. (b) Pseudocapacitance determination of InsP₆-PB-10 at 1 mV s⁻¹.

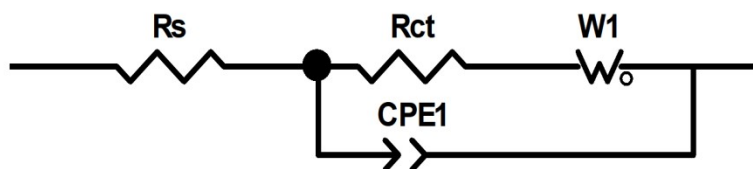


Fig. S11 The circuit model.

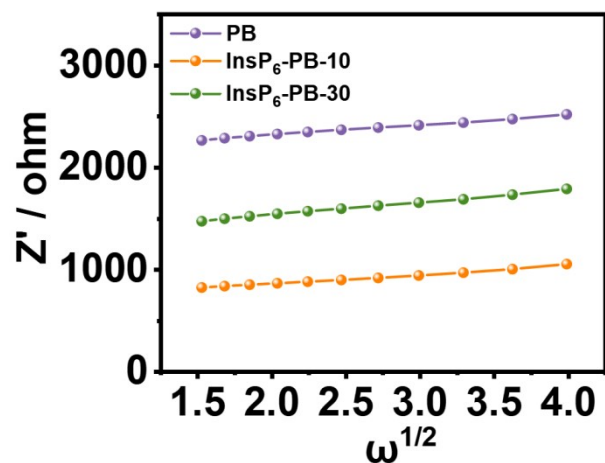


Figure S12. Z' vs. $\omega^{-1/2}$ plots.

Table S1 Rietveld-refined structural parameters for the PB sample.

Cubic, space group Fm-3m, a=b=c=10.211 Å, V=1064.63 Å ³ .					
Atom	x	y	z	Occupation	Uiso
Na	0.25000	0.25000	0.25000	0.2450	0.02957
Fe1	0.00000	0.00000	0.00000	0.8805	0.01274
Fe2	0.00000	0.00000	0.50000	1.0000	0.01143
C	0.00000	0.00000	0.17788	0.8805	0.01209
N	0.00000	0.00000	0.23859	0.8805	0.10545
O1	0.00000	0.00000	0.23859	0.0260	0.10565
O2	0.31059	0.31059	0.31059	0.0492	0.10085

Table S2 Rietveld-refined structural parameters for InsP₆-PB-10.

Cubic, space group Fm-3m, a=b=c=10.205 Å, V=1062.89 Å ³ .					
Atom	x	y	z	Occupation	Uiso
Na	0.25000	0.25000	0.25000	0.2850	0.02960
Fe1	0.00000	0.00000	0.00000	0.9694	0.00764
Fe2	0.00000	0.00000	0.50000	1.0000	0.01439
C	0.00000	0.00000	0.17788	0.9694	0.01254
N	0.00000	0.00000	0.23859	0.9694	0.10540
O1	0.00000	0.00000	0.23859	0.0065	0.10560
O2	0.31059	0.31059	0.31059	0.0123	0.10080

Table S3 Rietveld-refined structural parameters for InsP₆-PB-30.

Cubic, space group Fm-3m, a=b=c=10.209 Å, V=1064.25 Å³.					
Atom	x	y	z	Occupation	Uiso
Na	0.25000	0.25000	0.25000	0.2400	0.02960
Fe1	0.00000	0.00000	0.00000	0.9011	0.01270
Fe2	0.00000	0.00000	0.50000	1.0000	0.00715
C	0.00000	0.00000	0.17788	0.9011	0.01210
N	0.00000	0.00000	0.23859	0.9011	0.10540
O1	0.00000	0.00000	0.23859	0.0230	0.10565
O2	0.31059	0.31059	0.31059	0.0470	0.10085

Table S4 Composition analysis of PB, InsP₆-PB-10 and InsP₆-PB-30.

Sample	Na	Fe	C	N
PB	3.71%	34.73%	21.23%	24.55%
InsP ₆ -PB-10	3.91%	33.01%	21.71%	24.46%
InsP ₆ -PB-30	3.38%	32.71%	20.84%	23.34%

Table S5 The electrochemical performance of different types of chelating agents.

Samples	Reversible capacities	Rate capacities	Cycling performance	Reference
Acid–sodium acetate	113 mAh/g at 0.017 A/g	90 mAh/g at 0.85 A/g	81% after 500 cycles at 0.85 A/g	Ref.1 ¹
Benzoic acid	110 mAh/g at 0.1 A/g	95.9 mAh/g at 1 A/g	76% after 500 cycles at 1 A/g	Ref.2 ²
Sodium citrate	116 mAh/g at 0.01 A/g	70 mAh/g at 2 A/g	71% after 500 cycles at 0.1 A/g	Ref.3 ³
Sodium polyacrylate	140 mAh/g at 0.034 A/g	105 mAh/g at 5.1 A/g	94.6% after 1000 cycles at 1.7 A/g	Ref.4 ⁴
Sodium pyrophosphate	128.5 mAh/g at 0.034 A/g	117.6 mAh/g at 0.85 A/g	80.6% after 100 cycles at 0.17 A/g	Ref.5 ⁵
Cysteine	149.13 mAh/g at 0.025 A/g	60.09 mAh/g at 2 A/g	78.34% after 500 cycles at 0.5 A/g	Ref.6 ⁶
Na₂EDTA	120 mAh/g at 0.025 A/g	73 mAh/g at 1 A/g	80% after 1300 cycles at 0.5 A/g	Ref.7 ⁷
Sodium carboxymethyl cellulose	130 mAh/g at 0.05 A/g	116 mAh/g at 1 A/g	97.4% after 3000 cycles at 10 A/g	Ref.8 ⁸
Inositol hexakisphosphate	127 mAh/g at 0.017 A/g	87 mAh/g at 1.7 A/g	90% after 1000 cycles at 0.85 A/g	This work

Table S6 The electrochemical performance comparison between InsP₆-PB-10 and previously reported PB cathode

Samples	Reversible capacities	Rate capacities	Cycling performance	Reference
PB-B	113 mAh/g at 0.017 A/g	90 mAh/g at 0.85 A/g	81% after 500 cycles at 0.85 A/g	Ref.1 ¹
BTA-PB-1.6	110 mAh/g at 0.1 A/g	95.9 mAh/g at 1 A/g	76% after 500 cycles at 1 A/g	Ref.2 ²
PB-EG-5	142 mAh/g at 0.01 A/g	91.3 mAh/g at 1 A/g	70% after 1000 cycles at 1 A/g	Ref.9 ⁹
MnCoHCF/A-CNT	114 mAh/g at 0.03 A/g	94 mAh/g at 0.75 A/g	50.5% after 800 cycles at 0.75 A/g	Ref.10 ¹⁰
PBA-200	129 mAh/g at 0.01 A/g	82.3 mAh/g at 1.5 A/g	77% after 500 cycles at 0.5 A/g	Ref.11 ¹¹
InsP₆-PB-10	127 mAh/g at 0.017 A/g	87 mAh/g at 1.7 A/g	90% after 1000 cycles at 0.85 A/g	This work

Table S7 R_s and R_{ct} derived from Nyquist plots of as-prepared samples.

Sample	R _s (Ω)	R _{ct} (Ω)
PB	8.05	1828
InsP ₆ -PB-10	6.21	606
InsP ₆ -PB-30	5.76	1058

Reference

1. P. Wang, D. Zhu, Y. Li, Y. Liu, W. Zhao, Y. Zhang, S. Sun and S. Fang, Buffer solution induced highly crystalline sodium-rich Prussian blue for sodium storage, *Chem. Commun.*, 2024, **60**, 1603-1606.
2. C.-C. Wang, L.-L. Zhang, X.-Y. Fu, H.-B. Sun and X.-L. Yang, Hollow Layered Iron-Based Prussian Blue Cathode with Reduced Defects for High-Performance Sodium-Ion Batteries, *ACS Appl. Mater. Interfaces*, 2024, **16**, 18959–18970.
3. W. Wang, Y. Gang, Z. Hu, Z. Yan, W. Li, Y. Li, Q.-F. Gu, Z. Wang, S.-L. Chou, H.-K. Liu and S.-X. Dou, Reversible structural evolution of sodium-rich rhombohedral Prussian blue for sodium-ion batteries, *Nat. Commun.*, 2020, **11**, 980.
4. H. Ma, M. Jiang, Z. Hou, T. Li, X. Zhang, Y. Gao, J. Peng, Y. Li and J.-G. Wang, Medium-mediated high-crystalline Prussian blue toward exceptionally boosted sodium energy storage, *Energy Storage Mater.*, 2024, **70**, 103411.
5. J. Peng, J. Huang, Y. Gao, Y. Qiao, H. Dong, Y. Liu, L. Li, J. Wang, S. Dou and S. Chou, Defect-Healing Induced Monoclinic Iron-Based Prussian Blue Analogs as High-Performance Cathode Materials for Sodium-Ion Batteries, *Small*, 2023, **19**, 2300435.
6. Y. Wang, Z. Sun, J. Zhu, F. Ye, J. Zhu, R. Li and G. Chang, A highly efficient chelating agent assisted the synthesis of Prussian blue analogues as a cathode material for sodium ion batteries, *Colloid Surf. A-Physicochem. Eng. Asp.*, 2025, **716**, 136690.
7. X. Li, Y. Shang, D. Yan, L. Guo, S. Huang and H. Y. Yang, Topotactic Epitaxy Self-Assembly of Potassium Manganese Hexacyanoferrate Superstructures for Highly Reversible Sodium-Ion Batteries, *ACS Nano*, 2022, **16**, 453-461.
8. M. Jiang, Z. Hou, J. Wang, L. Ren, Y. Zhang and J.-G. Wang, Balanced coordination enables low-defect Prussian blue for superfast and ultrastable sodium energy storage, *Nano Energy*, 2022, **102**, 107708.
9. X. Xu, S. Zhu, C. Yang, Y. Wang, Z. Wu, J. Zheng, J. Wu and Y. Gao, A novel strategy for the reduction of coordinated water in Prussian blue analogues for their application as cathode materials for sodium-ion batteries, *J. Mater. Chem. A*, 2025, **13**, 11848-11860.
10. Y. Liu, Y. Zhang, H. Liu, B. Yao, Y. Zhong, Z. Wu, X. Wang and Z. Zhang, Boosting sodium storage capability of Prussian blue analogues through in-situ composite integration with carboxylated multi-walled carbon nanotubes, *Electrochim. Acta*, 2025, **524**, 146025.
11. J. Duan, Y. Sun, B. Li, P. Wu, Z. Li and J. Huang, Tailoring coordinated water in sodium-rich phase for high-performance Prussian blue cathodes, *Nanoscale*, 2025,

17, 24707-24714.